Please cite this article in press as: Huang et al., Mechanical force-promoted osteoclastic differentiation via periodontal ligament stem cell exosomal protein ANXA3, Stem Cell Reports (2022), https://doi.org/10.1016/j.stemcr.2022.06.006

Stem Cell Reports
Article
ISSCR
OPEN ACCESS

Mechanical force-promoted osteoclastic differentiation via periodontal ligament stem cell exosomal protein ANXA3

Hua-ming Huang,[1,2,3,5] Chun-Shan Han,[1,2,3,5] Sheng-jie Cui,[1,2,3] Yi-kun Zhou,[1,2,3] Tian-yi Xin,[1,2,3] Ting Zhang,[1,2,3] Song-biao Zhu,[4] Yan-heng Zhou,[1,2,3,*] and Rui-li Yang[1,2,3,*]

[1]Department of Orthodontics, Peking University School and Hospital of Stomatology, 22 Zhongguancun Avenue South, Haidian District, Beijing 100081, China
[2]National Clinical Research Center for Oral Diseases & National Engineering Laboratory for Digital and Material Technology of Stomatology, Haidian District, Beijing 100081, China
[3]Beijing Key Laboratory of Digital Stomatology, Haidian District, Beijing 100081, China
[4]MOE Key Laboratory of Bioinformatics, Center for Synthetic and Systematic Biology, School of Life Sciences, Tsinghua University, Beijing 100084, China
[5]These authors contributed equally
*Correspondence: yanhengzhou@vip.163.com (Y.-h.Z.), ruiliyang@bjmu.edu.cn or ruiliyangabc@163.com (R.-l.Y.)
https://doi.org/10.1016/j.stemcr.2022.06.006

SUMMARY

Exosomes play a critical role in intracellular communication. The biogenesis and function of exosomes are regulated by multiple biochemical factors. In the present study, we find that mechanical force promotes the biogenesis of exosomes derived from periodontal ligament stem cells (PDLSCs) and alters the exosomal proteome profile to induce osteoclastic differentiation. Mechanistically, mechanical force increases the level of exosomal proteins, especially annexin A3 (ANXA3), which facilitates exosome internalization to activate extracellular signal-regulated kinase (ERK), thus inducing osteoclast differentiation. Moreover, the infusion of exosomes derived from PDLSCs into mice promotes mechanical force-induced tooth movement and increases osteoclasts in the periodontal ligament. Collectively, this study demonstrates that mechanical force treatment promotes the biogenesis of exosomes from PDLSCs and increases exosomal protein ANXA3 to facilitate exosome internalization, which activates ERK phosphorylation, thus inducing osteoclast differentiation. Our findings shed light on new mechanisms for how mechanical force regulates the biology of exosomes and bone metabolism.

INTRODUCTION

Mechanical forces, including tension, compressive force, hydrostatic compressive force, and fluid shear stress, are usually applied throughout the development of multiple tissues (Moraes et al., 2011). The application of compressive force to normal bronchial epithelial cells that were grown at the air-liquid interface shrinks the lateral intercellular space surrounding the cells and triggers cellular signaling via autocrine binding (Tschumperlin et al., 2004). Furthermore, the adaptation of bone mass and architecture is driven by mechanical force (Teichtahl et al., 2015). When physiological magnitude mechanical loading is lost, reduced bone mineralization will lead to bone resorption and osteoporosis (Tamma et al., 2009). Notably, experiments *in vivo* have shown that mechanical force affects the function of mesenchymal stem cells (MSCs) in the process of force-induced bone reconstruction or cardiac injury remodeling (Liaw and Zimmermann, 2016; Papachroni et al., 2009). Mechanical forces *in vitro* also modulate the proliferation, differentiation, and paracrine activity of MSCs (Diaz et al., 2017; Le et al., 2016).

Exosomes are nanovesicles 30–150 nm in diameter that are secreted by various types of cells (Johnstone, 1992). They play a critical role in intercellular communication by transferring bioactive molecules between cells, such as lipids, proteins, and genetic information (Tkach and Thery, 2016). The regulation of exosome biogenesis is critical for intercellular communication (Zhang et al., 2015). A variety of microenvironmental factors, including hypoxia, inflammatory cytokines, and infectious agents, can promote exosome biogenesis (Colombo et al., 2014). Recently, cyclic stretch force has been found to induce cells to secrete exosomes, which inhibited IL-1β production in lipopolysaccharide-stimulated macrophages (Wang et al., 2019). However, the mechanism by which mechanical force modulates the biogenesis and function of exosomes from MSCs is still poorly understood.

Orthodontic tooth movement (OTM) is induced by mechanical forces and is promoted by the remodeling of periodontal ligament (PDL) and alveolar bone. The PDL is a dense fibrous connective tissue between the dental root and the alveolar bone that contributes to bone homeostasis and bone remodeling under mechanical stimulation. The PDL is exposed to endogenous mechanical stimulus derived from mastication and also suffers from exogenous mechanical loading, such as occlusal interference and orthodontic appliances. The force could be tension, fluid shear, compression, and hydrostatic force. During the process, the PDL produces a variety of components to regulate osteogenic- and osteoclastic-related signaling for the remodeling of periodontal tissue (Li et al., 2018a). PDL stem cells (PDLSCs) have been isolated and identified as the main MSCs in the PDL (Huang et al., 2018; Seo et al.,

Please cite this article in press as: Huang et al., Mechanical force-promoted osteoclastic differentiation via periodontal ligament stem cell exosomal protein ANXA3, Stem Cell Reports (2022), https://doi.org/10.1016/j.stemcr.2022.06.006

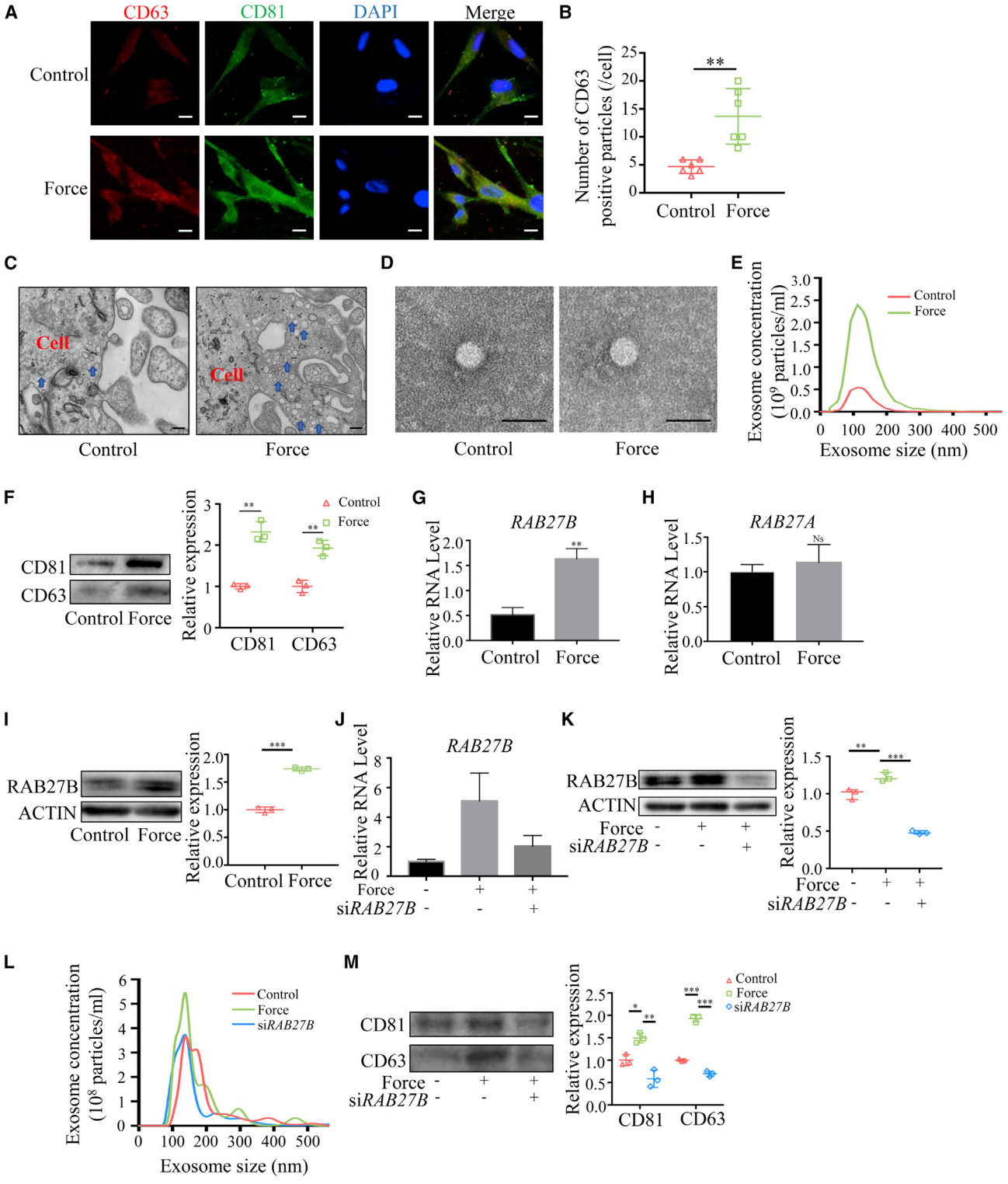

Figure 1. Compressive force promotes the biogenesis of exosomes derived from PDLSCs via RAB27B

(A and B) Immunofluorescent staining showed the expression of CD63 (red) and CD81 (green) in control or compressive force-primed PDLSCs (n = 6). Scale bars, 10 nm.

(legend continued on next page)

2004). Having immunomodulatory function and potential for the generation of cementum/PDL-like complex (Seo et al., 2004; Wada et al., 2009), PDLSCs are likely sensitive to mechanical loading and play critical roles in alveolar bone remodeling during OTM. During the response to mechanical force, PDLSCs produce a variety of inflammatory cytokines and chemokines to regulate osteogenic- and osteoclastic-related signaling for the remodeling of alveolar bone (Liu et al., 2017; Zhang et al., 2016). However, whether mechanical force induces PDLSCs to secrete exosomes to contribute to alveolar bone remodeling remains to be uncovered.

Herein, we demonstrate that mechanical force promotes the biogenesis of exosomes from PDLSCs through RAB27B. The exosomes primed by mechanical force showed superior capacity to induce osteoclast differentiation by upregulating the exosomal ANXA3 level, which facilitated exosome internalization to activate extracellular signal-regulated kinase (ERK) phosphorylation.

RESULTS

Mechanical force promotes the biogenesis of exosomes derived from PDLSCs via RAB27B

The effects of compressive force on the biogenesis of exosomes from PDLSCs were investigated. We applied 1.5 g/cm^2 static compressive force to PDLSCs for 24 h. Then, we did immunofluorescence staining using the exosome markers CD81 and CD63, and the results showed that the expression levels of CD81 and CD63 increased in force-primed PDLSCs compared with the control group (Figures 1A, 1B, and S1A), and more microvesicles were observed in the force-stimulated PDLSCs as analyzed by transmission electron microscopy (TEM; Figure 1C). The exosomes from the culture supernatant of PDLSCs were isolated, and their morphology and size were analyzed using TEM and nanoparticle tracking analysis (NTA). The results showed that PDLSC exosomes were round and ranged in size from 30 to 150 nm (Figures 1D and 1E). The number of exosomes induced by compressive force was nearly four times that of the control group, whereas the size of exosomes was not altered after force treatment (Figure 1E). In addition, compressive force treatment increased CD81 and CD63 expression in PDLSC exosomes (Figure 1F). RAB27 plays a crucial role in exosome biogenesis and secretion (Hessvik and Llorente, 2018; Kowal et al., 2014). We found that the expression of *RAB27B*, but not *RAB27A*, in the compressive force-stimulated PDLSCs was remarkably increased compared with the control group (Figures 1G and 1H). Western blot results confirmed that RAB27B expression was remarkably upregulated after force stimulation (Figure 1I). The increased number of exosomes and the upregulated expression of CD81 and CD63 in PDLSC exosomes induced by force were attenuated after *RAB27B* small interfering RNA (siRNA) treatment (Figures 1J–1M). These results indicate that compressive force increases the biogenesis of PDLSC exosomes through RAB27B.

Mechanical force promotes PDLSC exosomes to induce osteoclast differentiation

Exosomes derived from control or force-stimulated PDLSCs were applied to RAW264.7 macrophages with the soluble receptor activator of NF-κB ligand (RANKL), which is used to stimulate osteoclast differentiation, to figure out the effect of PDLSC exosomes on osteoclast differentiation. The results showed that exosome treatment promoted osteoclast differentiation substantially (Figures 2A and 2B), which was accompanied by increased expression levels of the osteoclast markers dendritic cell-specific transmembrane protein (*Dc-stamp*) and matrix metalloprotease 9 (*Mmp9*), as assessed by qPCR (Figures 2C and 2D). Moreover, exosomes from force-primed PDLSCs showed superior capability to promote osteoclast differentiation (Figures 2E–2H). However, exosomes failed to alter the osteogenic differentiation capacity of PDLSCs (Figure S1B). The results indicate that exosomes are able to induce and promote osteoclast differentiation.

(C) Transmission electron microscopy (TEM) images showing the microvesicles in control or compressive force-primed PDLSCs. Blue arrows indicate microvesicles. Scale bars, 200 nm.
(D) TEM images of exosomes purified from the culture supernatant of control or compressive force-primed PDLSCs. Scale bars, 50 nm.
(E) Nanoparticle tracking analysis (NTA) of exosomes derived from control or compressive force-primed PDLSCs.
(F) Western blot showing the expression of CD81 and CD63 in exosomes derived from control or compressive force-primed PDLSCs.
(G and H) PCR analysis showing the expression of *RAB27B* (G) and *RAB27A* (H) in control or compressive force-primed PDLSCs.
(I) Western blot showing the expression of RAB27B in control or compressive force-primed PDLSCs.
(J and K) PCR (J) and western blot (K) results showing the knockdown efficacy of *RAB27B* siRNA in PDLSCs (n = 3).
(L) NTA of exosomes derived from control PDLSCs, compressive force-primed PDLSCs, and PDLSCs treated with force and *RAB27B* siRNA.
(M) Western blot showing the expression of CD81 and CD63 in control PDLSCs, force-primed PDLSCs, and PDLSCs treated with force and *RAB27B* siRNA. Exosomes from equal quantities of PDLSCs for each group were used to load for western blot. The results are representative of data generated in three independent experiments.
Data are presented as the mean ± SD (*p < 0.05, **p < 0.01, ***p < 0.001). See also Figure S1.

Please cite this article in press as: Huang et al., Mechanical force-promoted osteoclastic differentiation via periodontal ligament stem cell exosomal protein ANXA3, Stem Cell Reports (2022), https://doi.org/10.1016/j.stemcr.2022.06.006

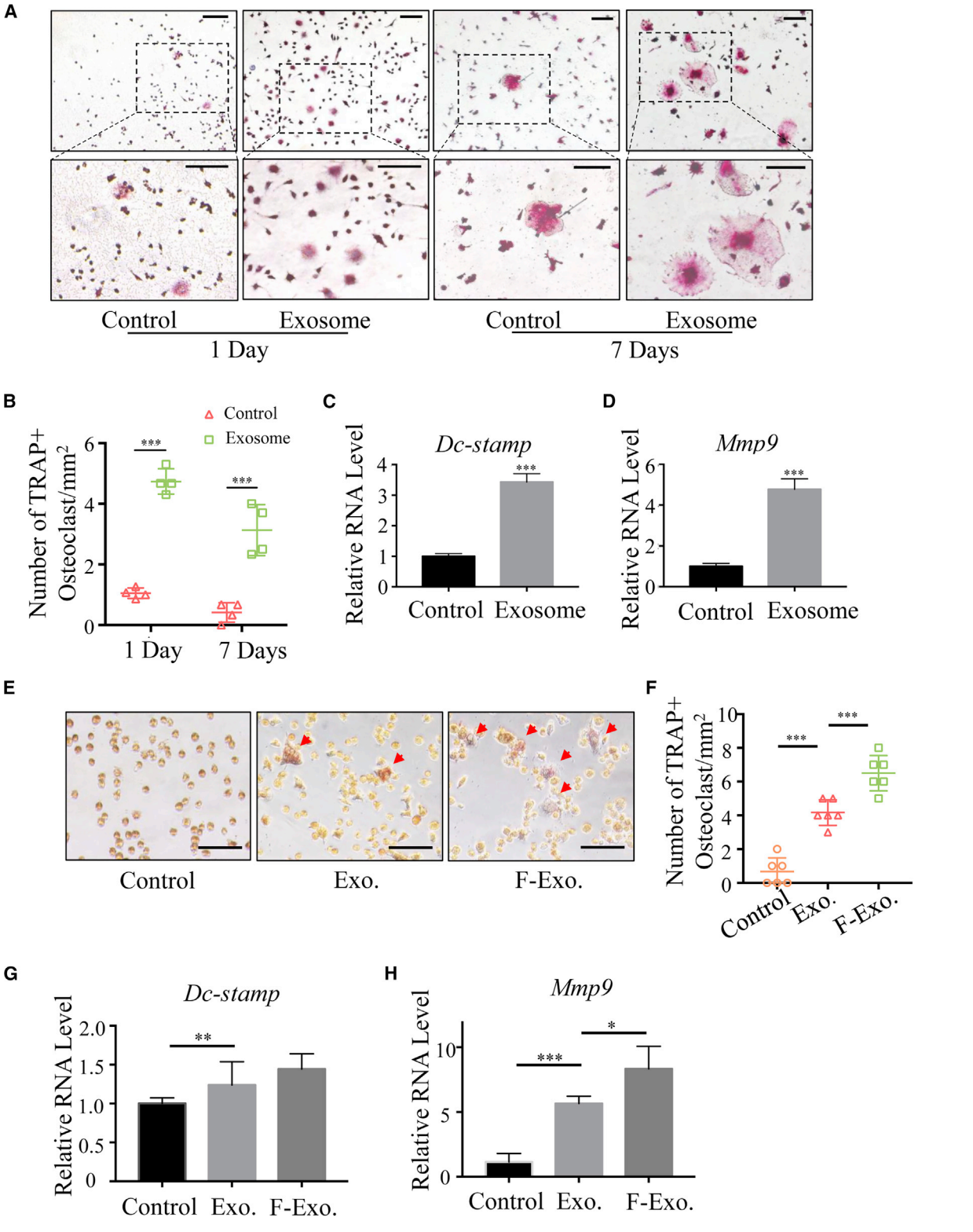

(legend on next page)

Exosomes are internalized by macrophages to induce osteoclast differentiation

Exosomes can be transferred from originating cells to recipient cells (Yi et al., 2020). We first tried to find out whether exosomes from PDLSCs can be internalized by RAW264.7 macrophages to explore the underlying mechanism by which exosomes induce osteoclast differentiation. PKH26-labeled exosomes were detected in the cytoplasm of macrophages after 1 h of treatment, and the intensity of red fluorescence increased after 3 h of treatment (Figures 3A and 3B). This finding indicates that exosomes were incorporated into the RAW264.7 macrophages in a time-dependent manner. The ERK pathway plays a pivotal role in osteoclast differentiation (Chinetti-Gbaguidi et al., 2017; Hotokezaka et al., 2002). PDLSC exosomes considerably upregulated ERK phosphorylation in macrophages compared with the control (Figures 3C and 3D). RAW264.7 cells were cultured with 5 μmol/L U0126 (ERK inhibitor) after exposure to exosomes to further explore the role of ERK signaling in osteoclast differentiation. The results showed that the osteoclast differentiation induced by exosomes was attenuated after U0126 treatment, accompanied by the decreased expression of *Dc-stamp* and *Mmp9* (Figure S2A; Figures 3E–3I). The proliferation of RAW264.7 macrophages was not affected by exosomes (Figure S2B). These results indicate that exosomes were internalized by macrophages and activated the phosphorylation of ERK to induce osteoclast differentiation.

Mechanical force enhances the enrichment of endocytic proteins in exosomes

The therapeutic effects of exosomes are mainly achieved by transferring various proteins or microRNAs (miRNAs) into recipient cells. Exosomes induced osteoclast differentiation by activating ERK phosphorylation, and exosomes showed superior capability to induce osteoclast differentiation. We performed mass spectrometry to determine whether exosome proteins play a role in osteoclast differentiation. We identified 194 proteins in exosomes (see Table S1 for complete list). Among them, 74 were shared by exosomes from control and compressive force-primed PDLSCs. We classified the upregulated proteins using gene ontology (GO) components, namely, biological processes, molecular processes, and cellular functions. The results showed that upregulated proteins were involved in phagocytic vesicles and endocytic vesicles (Figures 4A and 4B). Compared with the control exosomes, the upregulated proteins (fold change ≥ 2, $p < 0.01$; Figure S2C) in the force-primed PDLSC exosomes included the calcium ion-binding proteins annexin A3 (ANXA3) and annexin A6 (ANXA6), which are able to modulate ERK phosphorylation (Guo et al., 2021; Sun et al., 2020). Western blot results validated that the force pretreatment of PDLSCs increased the levels of ANXA3 and ANXA6 in exosomes (Figure 4C), but not in PDLSCs (Figure 4D). The results suggest that mechanical stimulation increases ANXA3 and ANXA6 aggregation in exosomes.

ANXA3 in exosomes activates ERK phosphorylation to promote osteoclast differentiation

ANXA3 and *ANXA6* siRNAs were used to pretreat PDLSCs, and then exosomes were isolated to verify the effects of ANXA3 and ANXA6 on osteoclast differentiation. The exosomes with low levels of ANXA3 or ANXA6 were used to treat RAW264.7 macrophages (Figure S2D; Figure 5A). The results showed that the efficacy of exosomes at inducing osteoclast differentiation was decreased by *ANXA3* siRNA but not by *ANXA6* siRNA pretreatment (Figures 5B–5D). The level of ERK phosphorylation in RAW264.7 macrophages promoted by exosomes was downregulated by *ANXA3* siRNA pretreatment (Figure 5E).

ANX can bind to Ca^{2+} ions and phospholipid membranes to form the surface of the cell membrane; therefore, it affects the endocytosis mediated by calcium ions (Bouter et al., 2015). We found that *ANXA3* siRNA pretreatment decreased the number of exosomes internalized by macrophages, assessed by immunofluorescence staining (Figure 5F), which suggests that ANXA3 is essential for the exosome internalization process.

Figure 2. Mechanical force promotes PDLSC exosome induction of osteoclast differentiation

(A) Tartrate-resistant acid phosphatase (TRAP) staining images of RAW264.7 macrophages treated with or without PDLSC exosomes for 1 and 7 days during osteoclast differentiation induced by soluble RANKL (n = 4). Scale bars, 200 μm.

(B) The number of TRAP-positive (TRAP+) osteoclast cells was increased in exosome group.

(C and D) Expression of *Dc-stamp* and *Mmp9* mRNA in RAW264.7 macrophages assessed by PCR after PDLSC exosome treatment for 1 day (n = 3).

(E) TRAP staining images of RAW264.7 macrophages treated with exosomes from control or force-primed PDLSCs for 1 day in the absence of soluble RANKL (n = 6). Red arrows indicate osteoclasts. Scale bars, 200 μm.

(F) The number of TRAP-positive (TRAP+) osteoclast cells was more in the F-Exo. group than that in the Exo. group. Exo., exosome; F-Exo., exosome derived from force-primed PDLSCs.

(G and H) Expression of *Dc-stamp* and *Mmp9* mRNA in RAW264.7 macrophages assessed by PCR after treatment with exosomes from control or force-primed PDLSCs for 1 day (n = 3). The results are representative of data generated from three independent experiments.

Data are presented as the mean ± SD (*p < 0.05, **p < 0.01, ***p < 0.001). See also Figure S1.

Please cite this article in press as: Huang et al., Mechanical force-promoted osteoclastic differentiation via periodontal ligament stem cell exosomal protein ANXA3, Stem Cell Reports (2022), https://doi.org/10.1016/j.stemcr.2022.06.006

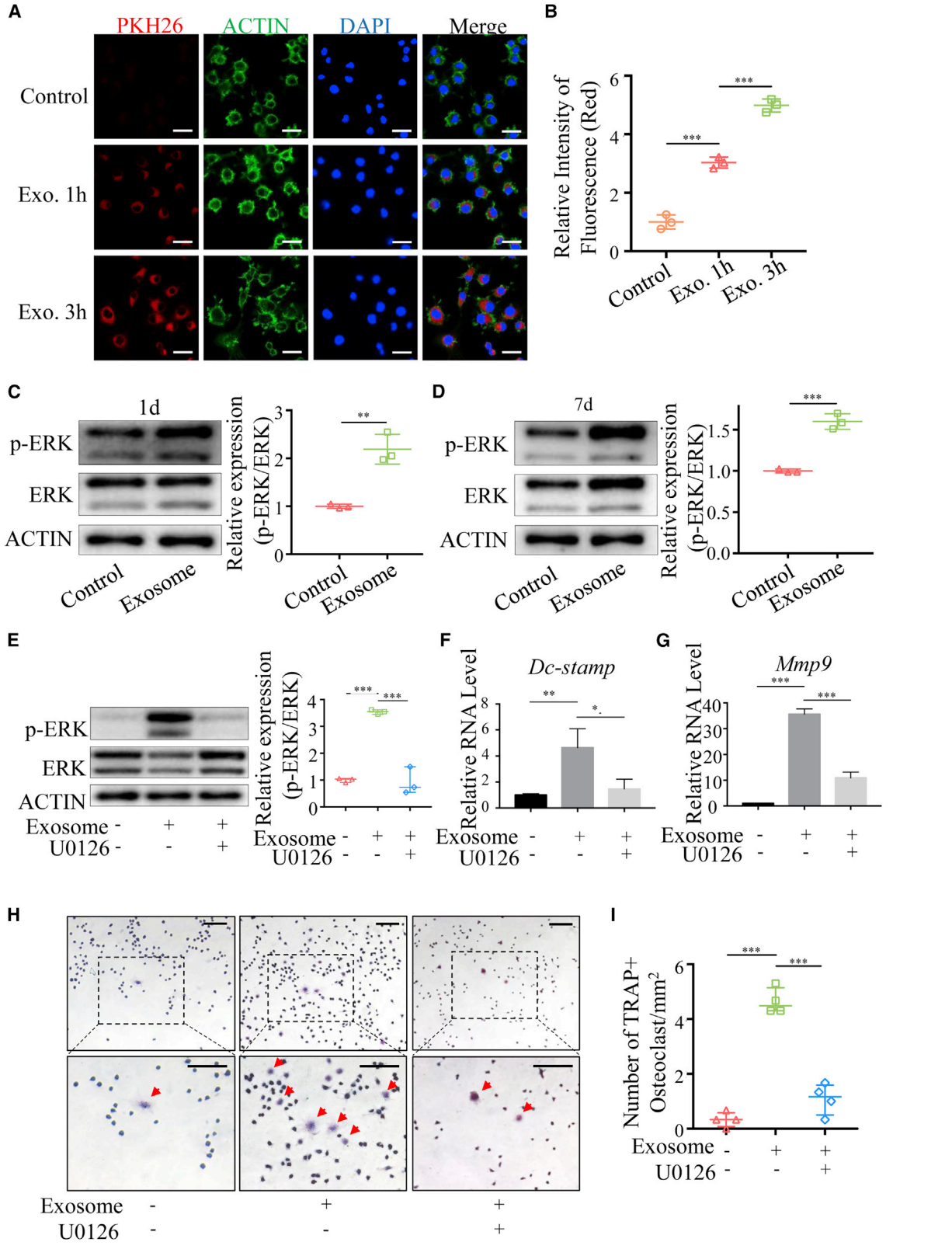

(legend on next page)

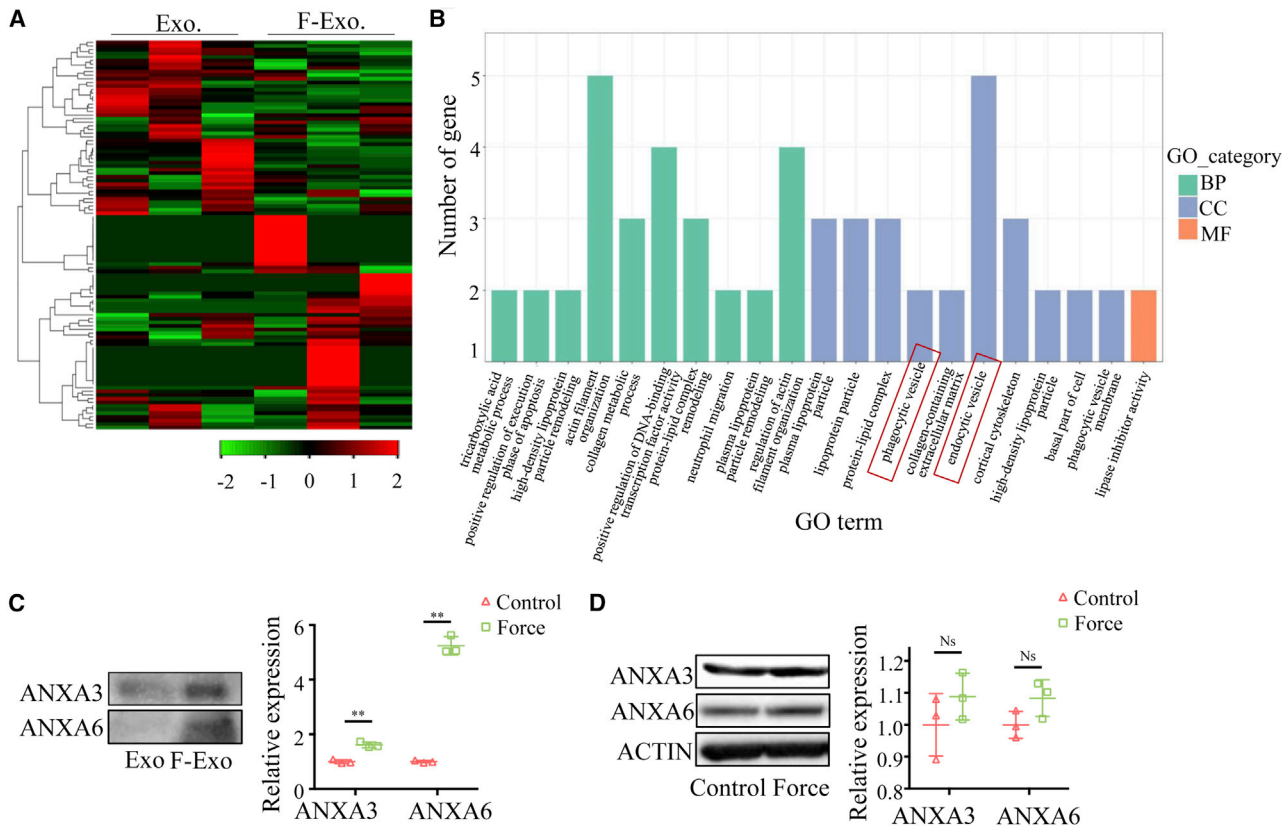

Figure 4. Mechanical force enhances the enrichment of endocytic related proteins in exosomes

(A) Exosomes derived from control or force-primed PDLSCs were collected and subjected to liquid chromatography-mass spectrometry (LC-MS) analysis. The identified differential proteins were used to perform heatmap analyses. The colors represent the protein concentration of each sample calculated by peak area normalization.

(B) Gene ontology (GO) analysis of the upregulated proteins. BP, biological process; CC, cellular function; MF, molecular process.

(C) Western blot showing the expression of ANXA3 and ANXA6 in exosomes derived from control and force-primed PDLSCs.

(D) Western blot showing the expression of ANXA3 and ANXA6 in control and force-primed PDLSCs. The same amount of exosomes from each group was used for the western blot. The results are representative of data generated from three independent experiments.

Data are presented as the mean ± SD (**p < 0.01). See also Figure S2 and Table S1.

To further verify the effects of ANXA3 on osteoclast differentiation, we used recombinant ANXA3 protein to treat RAW264.7 macrophages. The results showed that ANXA3 protein could induce osteoclast differentiation and upregulate the ERK phosphorylation in RAW264.7 macrophages (Figures 5G–5J). These results indicate that force

Figure 3. Exosomes are internalized by macrophages and activate ERK phosphorylation

(A) Immunofluorescence staining showing PKH26-labeled exosomes (red) in RAW264.7 macrophages after 1 and 3 h of treatment. Cells were stained with ACTIN (green) and DAPI (blue). Scale bars, 20 μm.

(B) The number of PKH26-labeled exosomes increased after 3 h of treatment. Exo., exosome.

(C and D) Western blots showing ERK phosphorylation in RAW264.7 macrophages after being treated with exosomes for 1 and 7 days.

(E) Western blot showing the phosphorylation of ERK in RAW264.7 macrophages after being treated with exosomes for 1 day with ERK inhibition (U0126) or not.

(F and G) PCR analysis showing that U0126 downregulated the expression of *Dc-stamp* and *Mmp9* that was increased by exosome treatment for 1 day.

(H) TRAP staining showing that the increased number of TRAP-positive (TRAP+) osteoclasts induced by PDLSC exosomes for 1 day was decreased after using U0126 (n = 4). Scale bars, 200 μm. Red arrows indicate osteoclasts.

(I) The increased number of TRAP-positive (TRAP+) osteoclast cells was attenuated after U0126 treatment. The results are representative of data generated from three independent experiments.

Data are presented as the mean ± SD (*p < 0.05, **p < 0.01, ***p < 0.001). See also Figure S2.

Please cite this article in press as: Huang et al., Mechanical force-promoted osteoclastic differentiation via periodontal ligament stem cell exosomal protein ANXA3, Stem Cell Reports (2022), https://doi.org/10.1016/j.stemcr.2022.06.006

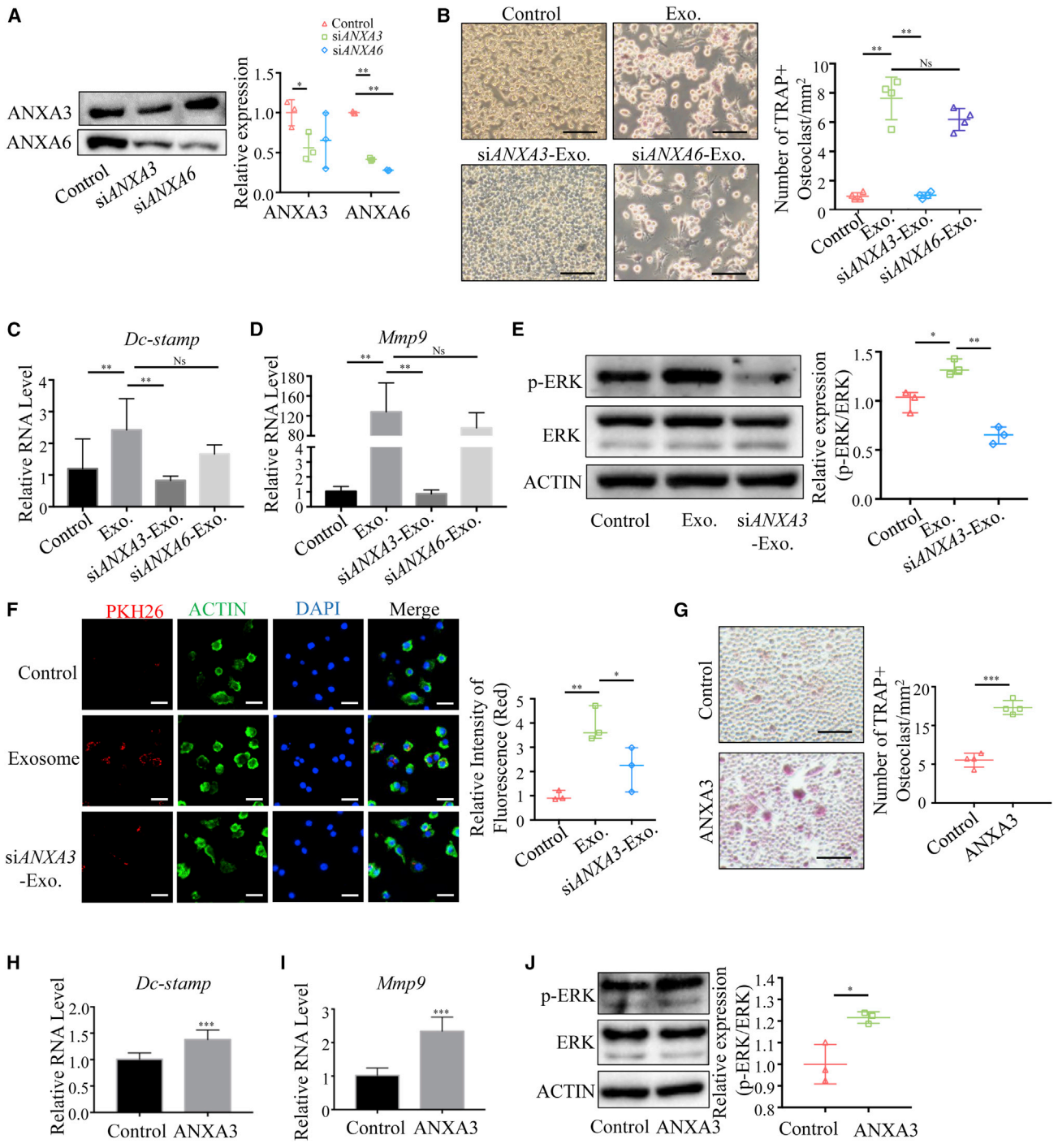

Figure 5. Exosomal ANXA3 activates ERK phosphorylation to promote osteoclast differentiation

(A) Western blot showing the expression of ANXA3 and ANXA6 in exosomes derived from PDLSCs treated with control siRNA, *ANXA3* siRNA, or *ANXA6* siRNA.

(B) TRAP staining images of RAW264.7 macrophages treated with PDLSC exosomes pretreated with control siRNA, *ANXA3* siRNA, or *ANXA6* siRNA (n = 5). Scale bars, 200 μm.

(C and D) Expression of *Dc-stamp* and *Mmp9* mRNA in RAW264.7 macrophages treated with PDLSC exosomes pretreated with control siRNA, *ANXA3* siRNA, or *ANXA6* siRNA, assessed by PCR.

(legend continued on next page)

pretreatment increases ANXA3 level in exosomes, which activates ERK phosphorylation in RAW264.7 macrophages and promotes osteoclast differentiation.

PDLSC exosomes enhance mechanical force-induced tooth movement

Exosomes play a crucial role in variety of physical and pathological processes (Kukita et al., 2004). We established an animal model of mechanical force-induced tooth movement and found that the expression of exosome marker CD63 in periodontal tissue was elevated after force treatment, which suggests that compressive force increases exosome biogenesis *in vivo* (Figures 6A and 6B). We injected PDLSC exosomes into mice intravenously on day 0 during tooth movement to further examine the effects of PDLSC exosomes on osteoclast differentiation. The results showed that, compared with the control group, PDLSC exosomes increased the distance of tooth movement (Figures 6C–6G). Tartrate-resistant acid phosphatase (TRAP) staining results showed that the injection of PDLSC exosomes increased the number of force-enhanced TRAP-positive osteoclasts on the compressive side of PDL and alveolar bone (Figures 6I and 6J), while the number of osteocalcin-positive osteoblasts slightly increased on the tension side of the PDLSC exosome infusion group (Figure S3A). In addition, the length of the distal buccal root of the first molar showed no remarkable change after exosome infusion compared with the control group (Figure S3B). The results indicate that exosome infusion could promote force induced osteoclast differentiation and bone remodeling.

Inhibition of ERK signaling blocks tooth movement induced by exosome infusion

U0126 was injected into mice on day 0 during tooth movement to verify the role of ERK signaling in exosome-induced osteoclast differentiation (Figure 7A). The results showed that the increased distance of tooth movement induced by PDLSC exosomes was attenuated after U0126 treatment in mice (Figures 7B–7F). The number of TRAP-positive osteoclasts on the compressive side, which was up-regulated by exosomes, was decreased after U0126 treatment (Figures 7G and 7H). These results confirm that PDLSC exosomes promote osteoclast differentiation and tooth movement via the ERK signaling pathway.

DISCUSSION

Exosomes have become a potential cell-free therapeutic tool for various diseases (Mendt et al., 2019). As the therapeutic effect of exosomes is dose dependent, increasing the number and properties of exosomes is an urgent medical need. Several researchers have investigated the use of different biomedical molecules, such as cytokines; hypoxia; and gene modification to improve the production and function of exosomes. The amount of tissue factor in bronchoalveolar lavage fluid from patients with asthma was five times greater than that of healthy controls. Airway epithelium that suffers from pressure, such as compressive stress, during bronchoconstriction in asthma produces more exosomes (Park et al., 2012). Mechanical stress induces the release of exosomes containing the angiotensin 2 type 1 receptor *in vitro* under hypotonic conditions and *in vivo* with pressure overload (Pironti et al., 2015). In another study, the extracellular vesicles derived from 24 h mechanical stress-treated cardiomyocytes were present at increased numbers and were of larger size (Yuan et al., 2018). Our results showed that the number of exosomes from PDLSCs induced by compressive force was nearly four times that of the control group. The size of the exosomes was not altered after compressive force treatment. In addition, our results showed that exosomes derived from compressive force-primed PDLSCs showed higher efficacy at inducing osteoclast differentiation compared with the control exosomes. These data indicate that force may be an alternative to enhance the therapeutic effect of exosomes. Further investigation is needed to explore a more efficient strategy to promote the properties of exosomes.

Exosome secretion is a multi-step process regulated by a series of molecules. Studies showed that Rab GTPases and SNARE proteins (SNAP-23 and VAMP7) are involved in

(E) Western blot showing ERK phosphorylation in RAW264.7 macrophages after being treated with PDLSC exosomes pretreated with control siRNA or *ANXA3* siRNA.
(F) Immunofluorescence staining showing PKH26-labeled exosomes (red) derived from PDLSCs treated with control siRNA or *ANXA3* siRNA in RAW264.7 macrophages after 3 h of treatment. Cells were stained with ACTIN (green) and DAPI (blue). Scale bars, 20 μm.
(G) TRAP staining images of RAW264.7 macrophages treated with ANXA3 protein for 1 day in the absence of soluble RANKL. Scale bars, 200 μm.
(H and I) Expression of *Dc-stamp* and *Mmp9* mRNA in RAW264.7 macrophages assessed by PCR after treatment with ANXA3 protein.
(J) Western blot showing ERK phosphorylation in RAW264.7 macrophages after being treated with ANXA3 protein or not. Exo., exosome; si*ANXA3*-Exo. and si*ANXA6*-Exo., exosomes derived from PDLSCs treated with *ANXA3* siRNA or *ANXA6* siRNA. The same amount of exosomes from each group was used for western blots. The results are representative of data generated from three independent experiments. Data are presented as the mean ± SD (*p < 0.05, **p < 0.01, ***p < 0.001). See also Figure S2.

Please cite this article in press as: Huang et al., Mechanical force-promoted osteoclastic differentiation via periodontal ligament stem cell exosomal protein ANXA3, Stem Cell Reports (2022), https://doi.org/10.1016/j.stemcr.2022.06.006

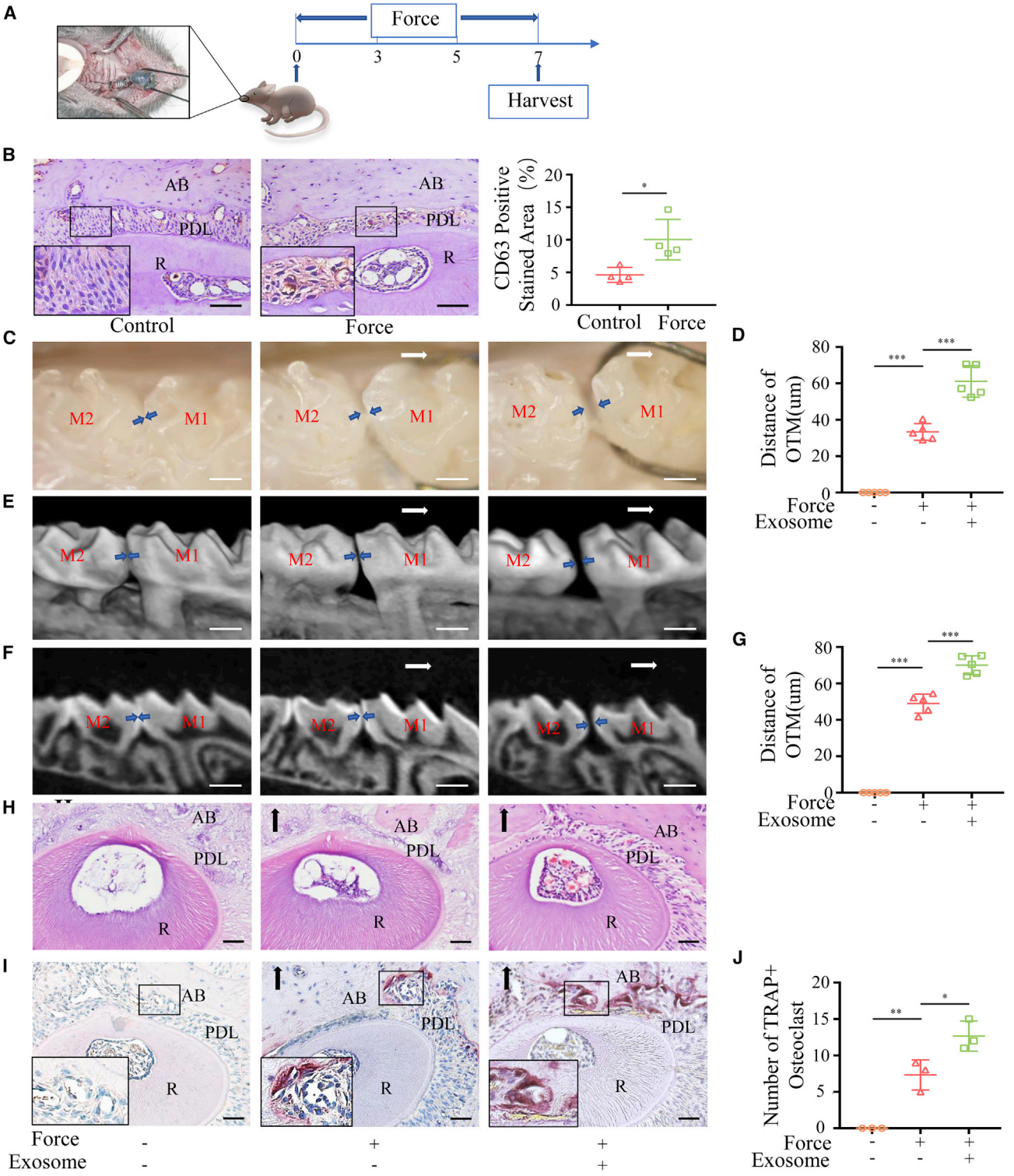

Figure 6. PDLSC exosomes enhance mechanical force-induced tooth movement

(A) Schema of the tooth movement. Mechanical force was applied to mice in each group for 7 days.

(B) Immunohistochemical staining showing that CD63 expression on the compression side of periodontal tissue was elevated after force (n = 4).

(legend continued on next page)

exosome secretion (Hsu et al., 2010; Wei et al., 2017). Rab GTPases influence docking as well as fusion processes and play a critical role in the regulation of extracellular microvesicle (MVB) transmission (Li et al., 2018b). RAB27A and RAB27B have common functions in the docking of MVBs on plasma membrane, but the two RAB27 isoforms have different roles in the exosomal pathway (Ostrowski et al., 2010). In our study, we found that the expression of RAB27B, but not RAB27A, was upregulated after force stimulation, which suggests that RAB27B may be more sensitive to mechanical forces than RAB27A. Further research on the function of RAB27B after mechanical force treatment is needed to elucidate the molecular mechanisms of mechanical force-induced exosome secretion.

Bone remodeling gives rise to a dynamic bone structure through a balance between bone formation by osteoblasts and resorption by osteoclasts, which allows the accommodation of bones to dynamic mechanical forces. Mechanical forces are indispensable for bone homeostasis; bone formation, resorption, and adaptation are dependent on mechanical signals (Wang et al., 2022). Prolonged periods of disuse that occur with therapeutic bed rest, paralysis, and limb amputation can substantially reduce the mechanical stress placed on the bone, thus resulting in disuse osteoporosis. During spaceflight, an extreme form of disuse, bone loss is accelerated due to increased bone resorption and decreased bone formation (Alexandre and Vico, 2011; LeBlanc et al., 2007). In addition, studies have suggested that abnormal mechanical loading activates osteoclast activity and increased bone resorption in subchondral bone, which is associated with the pathogenesis of osteoarthritis (Karsdal et al., 2014). Our results showed that mechanical force regulates bone remodeling through exosome release, suggesting that exosome release could be a new mechanism by which the body senses and transduces mechanical forces to regulate bone remodeling.

Annexins are a key subgroup of calcium-ion-binding proteins, involved in the regulation of membrane trafficking, cell adhesion, and immune responses. ANXAs are involved in homeostasis in bone cells (Balcerzak et al., 2003), and ANXA2 has been suggested to stimulate osteoclast formation (Menaa et al., 1999). Our results showed that ANXA3 activates the ERK signaling pathways to induce osteoclast differentiation; however, ANXA6 failed to alter osteoclast differentiation (Guo et al., 2021; Sun et al., 2020). The levels of both ANXA3 and ANXA6 in exosomes were decreased after *ANXA3* siRNA treatment. These results indicate that different proteins in the ANXA family may play different roles. As far as we know, this study is the first to illustrate that compressive force promotes exosomes to induce osteoclast differentiation, which is mediated by ANXA3 in exosomes. The composition of exosomes differs depending on the source and the cell status (Ferguson and Nguyen, 2016). For example, active hematopoiesis increased the exosomal release of PRDX2 from erythroblastic cells, which induced osteoclast formation (Sadvakassova et al., 2021). Moreover, the exosomal release of L-plastin was important for breast cancer-induced osteoclast formation, as inhibition of exosomal release reduced the osteoclastogenic potential of breast cancer cells (Tiedemann et al., 2019). Whether other proteins or miRNAs were altered in exosomes derived from different primed MSCs and the underlying mechanism needs to be further studied.

Other than their role in intercellular signaling, exosomes have been known to function in cell-cell communications and as drug delivery vehicles. Exosomes regulate intercellular communication by serving as vehicles to transfer various cellular constituents through endocytosis. The lipid and protein content of vesicles may affect the endocytosis process and their tropism to specific organs (Murphy et al., 2019). For example, the lipid composition of extracellular vehicles (EVs) influences the cellular uptake of EVs by macrophages (Matsumoto et al., 2017). Similarly, EVs containing integrin alpha4 and Tspan8 were more preferentially taken up by pancreatic cells (Rana et al., 2012). Here, we showed that ANXA3 expression in exosomes could promote exosome accumulation in macrophages. The ANXA3 level in exosomes from PDLSCs was enhanced by mechanical force treatment. These results indicate that mechanical force may be one alternative strategy to enhance the drug delivery efficacy of EVs. However, the specific mechanisms for how ANXA3 protein regulates the endocytosis process need further investigation.

(C–G) Injection of PDLSC exosomes was performed on the first day of tooth movement (day 0). The occlusal view (C and D) and three-dimensional reconstruction (E), as well as the sagittal view (F and G) by micro-computed tomography (micro-CT), of the first and second molars show that PDLSC exosomes increased the OTM distance compared with the control group (n = 5).
(H) Hematoxylin and eosin (H&E) staining on the compressive side of the distal root of the maxillary first molar.
(I and J) TRAP staining on the compressive side of the distal root of the maxillary first molar. The number of TRAP-positive (TRAP+) osteoclast cells was upregulated in the exosome group (n = 3). AB, alveolar bone; R, root; M1, first molar; M2, second molar. Blue arrows indicate the OTM distance. White and black arrows indicate the direction of the mechanical force. Scale bars, 100 μm (C, E, and F) and 200 μm (B, H, and I). The results are representative of data generated from three independent experiments.
Data are presented as the mean ± SD (*p < 0.05, **p < 0.01, ***p < 0.001). See also Figure S3.

Please cite this article in press as: Huang et al., Mechanical force-promoted osteoclastic differentiation via periodontal ligament stem cell exosomal protein ANXA3, Stem Cell Reports (2022), https://doi.org/10.1016/j.stemcr.2022.06.006

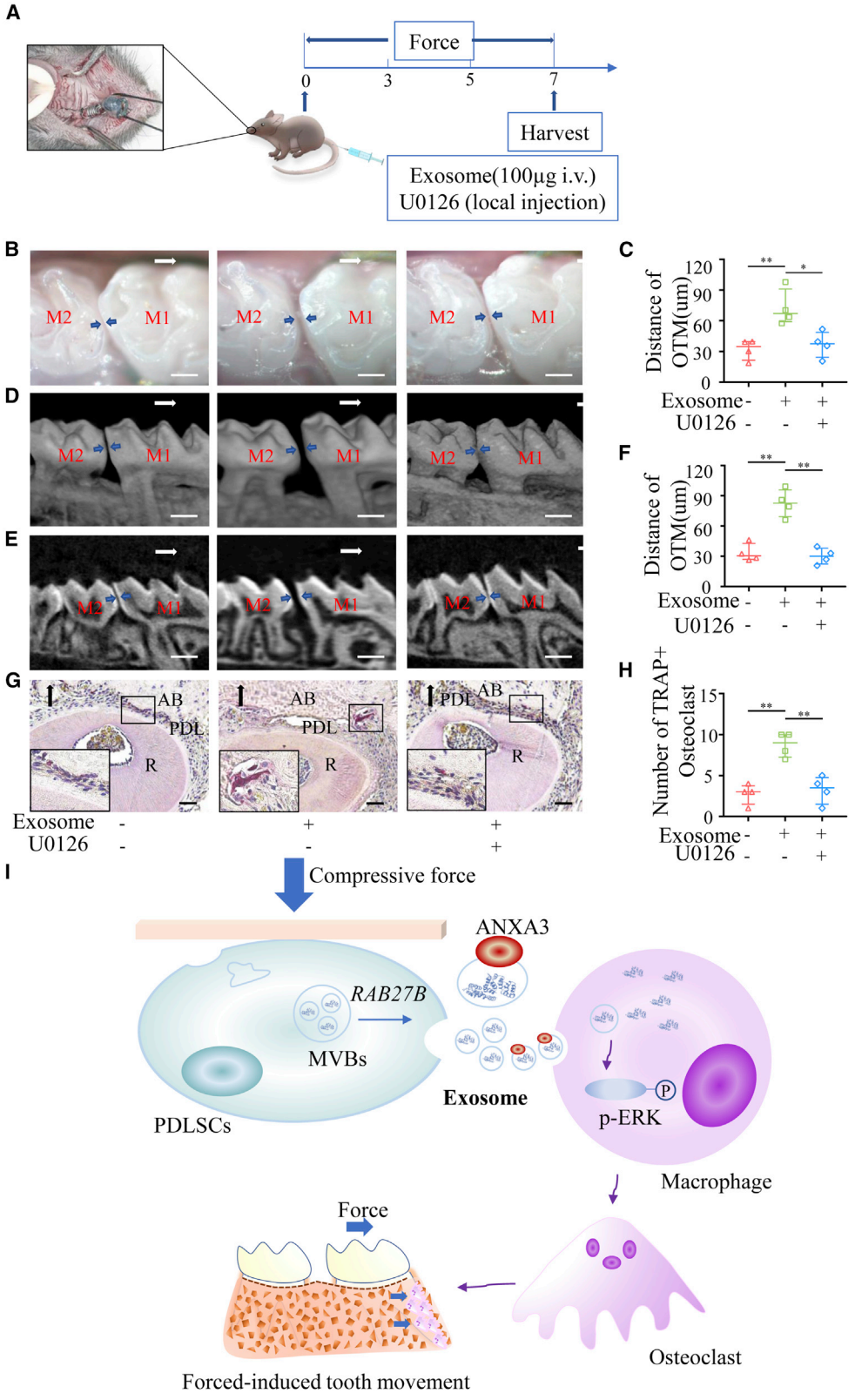

(legend on next page)

A variety of signaling pathways, such as NF-κB, p38, c-Jun N-terminal kinase, and Src, regulate osteoclast differentiation (Boyle et al., 2003). In the present study, we found that PDLSC exosomes activated the ERK pathway to promote osteoclast differentiation and tooth movement. Whether other pathways are regulated by PDLSC exosomes needs to be further studied.

In summary, our study showed that compressive force promotes the biogenesis of exosomes from PDLSCs through RAB27B. Compressive force-primed PDLSC exosomes have a superior capability to promote osteoclast differentiation, which is mediated by increasing the expression of ANXA3. Mechanically, ANXA3 in exosomes induces osteoclast differentiation by activating the phosphorylation of ERK (Figure 7I). Our research highlights a new property of mechanical force in regulating exosome biogenesis and function and reveals that exosomes may be a promising alternative for targeting bone remodeling.

EXPERIMENTAL PROCEDURES

Ethics approval

This study was approved by the Animal Use and Care Committee of Peking University (approval LA2019-92). All institutional and national guidelines for the care and use of laboratory animals were followed.

Cell culture and treatment

The protocols for obtaining human tissue have been previously described (Liu et al., 2017) and were performed after obtaining informed consent from participants and approval from the Peking University Ethical Guide (PKUSSIRB-201311103). PDLSCs were isolated from the healthy donors' extracted premolars as previously described (Liu et al., 2017) and cultured at 37°C with 5% CO_2 and the alpha modification of Eagle's medium (α-MEM) containing 15% fetal bovine serum (FBS; Gibco, Carlsbad, CA). Static compressive force application on PDLSCs was performed using a layer of glass and metal weights placed on the top of the cell layer at 80% confluence in plates. We applied 1.5 g/cm^2 compressive force on PDLSCs for 24 h, which was indicated as an appropriate force to induce a physiological response in PDLSCs (Liu et al., 2017). PDLSCs were observed with a transmission electron microscope (FEI Tecnai Spirit 120 kV).

Murine macrophage RAW264.7 cells were purchased from the National Infrastructure of Cell Line Resource (Beijing, China) and cultured with RPMI 1640 medium containing 15% FBS at 37°C with 5% CO_2. For osteoclast differentiation, RAW264.7 cells were seeded in six-well dishes at a density of 5×10^5 cells per well, cultured overnight, and then treated with 50 ng/mL soluble RANKL. At the same time, RAW264.7 cells were treated with 50 μg/mL PDLSC exosomes or control phosphate-buffered saline (PBS) for 1 or 7 days. For the signaling inhibition assay, the RAW264.7 cells were pretreated with inhibitors of ERK (U0126, 5 μM; Merck Millipore) or control vehicle (DMSO) for 2 h and then treated with PDLSC exosomes for 1 day.

Isolation, analysis, and labeling of exosomes

Exosomes were isolated from PDLSCs cultured in α-MEM with exosome-free serum (centrifuged at 120,000*g* for 70 min) for 48 h. The culture supernatant was collected and exosomes were isolated using an exosome isolation kit (System Biosciences) or ultracentrifugation according to previously described standard methods (Jiang et al., 2017). Optima MAX-XP (Beckman Coulter, USA) was used to perform ultracentrifugation experiments. The final pellet was resuspended in PBS for further analyses. The protein amount in exosomes was quantified by bicinchoninic acid assay. TEM (JEM-1400PLUS, Japan) was performed to observe exosomes. To quantify exosomes, NTA was performed at Shanghai Biotechnology (Shanghai, China) with the ZetaView PMX 110 (Malvern Instruments, UK). PKH-26 (Sigma-Aldrich, USA) was used for exosome labeling according to the instructions of the manufacturer.

Transmission electron microscopy

Exosomes were fixed in 2% paraformaldehyde, washed, and loaded onto Formvar-carbon-coated grids. After washing, exosomes were postfixed in 2% glutaraldehyde for 2 min, washed, and contrasted in 2% phosphotungstic acid for 5 min. Samples were washed,

Figure 7. Inhibition of ERK signaling blocked tooth movement induced by exosome infusion

(A) Schema of the injection of ERK inhibitor U0126. Mechanical force was applied to the mice in each group for 7 days. The injections of PDLSC exosomes and U0126 were performed on the first day of tooth movement. i.v., intravenously.

(B–F) The occlusal view (B and C) and three-dimensional reconstruction (D), as well as the sagittal view (E and F) by micro-CT, of the first and second molars from mice induced by PDLSC exosomes. The OTM distance was attenuated after U0126 was injected intravenously (n = 4).

(G and H) TRAP staining on the compressive side of the distal root of the maxillary first molar. The number of TRAP-positive (TRAP+) osteoclast cells upregulated by exosomes was downregulated after U0126 treatment (n = 4). AB, alveolar bone; R, root; M1, first molar; M2, second molar. Blue arrows indicate the OTM distance. White and black arrows indicate the direction of the mechanical force. Scale bars, 100 μm (B, D, and E) and 200 μm (G). The results are representative of data generated from three independent experiments. Data are presented as the mean ± SD (*p < 0.05, **p < 0.01).

(I) Schematic diagram. Compressive force promotes the biogenesis of exosomes from PDLSCs through RAB27B. Compressive force-primed PDLSC exosomes have a superior ability to promote osteoclast differentiation, which is mediated by increasing the level of exosomal ANXA3. Mechanically, exosomal ANXA3 facilitates the internalization of exosomes by macrophages to induce osteoclast differentiation by activating ERK phosphorylation, thereby accelerating the process of tooth movement. MVBs, extracellular microvesicles.

dried, and examined using an electron microscope (JEM-1400PLUS, Japan).

For cells, control and force-stimulated PDLSCs were collected by centrifugation and fixed with 2.5% glutaraldehyde overnight and then fixed with 1% osmium tetraoxide for 2 h, dehydrated in a graded series of ethanol concentrations, and embedded in SPIPON812 resin and polymerized. The block was sectioned by microtome (Leica EM UC6). The ultrathin sections of approximately 70 nm were mounted on copper grids, uranyl acetate and lead citrate were used to stain them, and they were examined and photographed with an FEI Tecnai Spirit TEM (FEI Tecnai Spirit 120 kV).

Nanoparticle tracking analysis

NTA was performed with the ZetaView PMX 110 (Particle Metrix, Meerbusch, Germany). Purified exosomes were diluted with PBS to measure the particle size and concentration. The corresponding software, ZetaView 8.04.02, was used to analyze the data. To convert the yield from concentration to an accurate number of particles, dilution factors and resuspension volumes were used.

Exosome proteome analysis by mass spectrometry

For proteomic analysis of exosomes, exosome samples were lysed by sodium dodecyl sulfate. Five micrograms of exosome proteins per group was isolated using SDS-PAGE followed by Coomassie blue staining and destaining. The whole lane corresponding to each sample was cut into 1 × 1 mm cubes using a clean scalpel. Then the gels were destained, reduced with dithiothreitol solution (5 mM dithiothreitol in 50 mM ammonium bicarbonate), and alkylated with iodoacetamide solution (11 mM iodoacetamide in 50 mM ammonium bicarbonate). Then trypsin solution was added to the gels for digestion overnight at 37°C. The supernatant containing the digested peptides was transferred into a clean tube for liquid chromatography-tandem mass spectrometry (LC-MS/MS) analysis. The raw data of mass spectrometry were searched against the UniProt human proteome by using the Proteome Discoverer software (version 1.4; Thermo Scientific). The parameters for database searching were static modifications of carbamidomethylation (+57.021 Da) on cysteine; dynamic modification of oxidation (+15.995 Da) on methionine; no more than two missed cleavages were allowed; the mass tolerances of precursors and fragments were 20 ppm and 0.02 Da, respectively; only peptides with false discovery rate below 1% were considered as high-confidence hits; and only unique peptides were used for protein quantification.

Western blot analysis

Cells and purified exosomes were lysed using a protein extraction kit (RIPA cocktail; Thermo). The same amounts of whole-cell lysates or exosomal proteins for each group were loaded for western blot. For analyzing the amount of exosomes (CD63 and CD81), we used exosomes from equal quantities of PDLSCs for each group to load in the western blot. SDS-PAGE was applied to isolate the same amount of proteins, and the proteins were transferred onto a polyvinylidene fluoride membrane. The membranes were blocked with 5% non-fat milk and 0.1% Tween 20 for 1 h and incubated with CD63 (1:1,000, A5271; ABclonal Technology); CD81 (1:500, sc-166029), annexin III (1:1,000, sc-390700), annexin VI (1:1,000, sc-271859), and β-actin (1:10,000, sc-8432) (Santa Cruz Biotechnology); and ERK (1:1,000, 4695S) and p-ERK (1:1,000, 4370S) (Cell Signaling Technology) primary antibodies at 4°C overnight. The blots were delivered by a horseradish peroxidase (HRP)-conjugated secondary antibody and subjected to enhanced chemiluminescence detection. Quantitative analysis was performed by ImageLab software provided by the manufacturer (Bio-Rad).

Immunofluorescence staining

Immunofluorescence staining was used to show the expression of CD81 and CD63 in PDLSCs and the PKH26 exosomes in RAW264.7 macrophages. Cells were fixed in 4% paraformaldehyde and washed with PBS. The PDLSCs were stained by primary antibodies of anti-CD81 (1:200, Santa Cruz Biotechnology) and CD63 (1:200, ABclonal Technology). RAW264.7 macrophages with or without PKH26 exosomes were stained with fluorescently labeled phalloidin (Oregon Green, Invitrogen, USA). Nuclei were counterstained with 4′,6-diamidino-2-phenylindole. Confocal microscopic images were processed with LSM 5 release 4.2 software after acquisition by a laser-scanning microscope (LSM 510; Zeiss).

An experimental animal model of mechanical loading

Following the Animal Use and Care Committee of Peking University approval (LA2019-92), 8-week-old adult C57BL/6 mice (male, 20–25 g) were used in our study. Mechanical force was applied following a previously described method (Liu et al., 2017). In short, a nickel-titanium coil spring (diameter, 1 mm; wire size, 0.2 mm; length, 1 mm) was bonded between the left first maxillary molar and the incisors to deliver a constant force of nearly 30 g for 7 days. The contralateral first molar was used as a control. At the same time, mice were administered intravenously with either purified PDLSC exosomes (100 μg) suspended in 200 μL PBS or control PBS as reported before (Liu et al., 2017). To specifically identify the role of ERK signaling in tooth movement induced by exosome infusion, mice were randomly intraperitoneally or locally injected with ERK inhibition (locally, 50 nM; Merck Millipore) or control DMSO after PDLSC exosome infusion.

Micro-computed tomography analysis

The mice were sacrificed after force was applied for 7 days. The entire maxillae were removed. The occlusal view of the maxillae was recorded by a stereomicroscope (SWZ1000; Nikon, Japan). The distance of tooth movement was measured as previously described (He et al., 2015; Liu et al., 2017). Briefly, the distance was measured between the tangent to the distal edge of the first molar and the tangent to the mesial edge of the second molar. Then, the maxillae of mice were scanned using a micro-computed tomography (micro-CT) system (SkyScan, Bruker, Germany, 860 μA, 55 kV, 12.5 μm pixel size). Radiographs were reconstructed and analyzed with CTan and CTvox software (Bruker). For the femur, the region of interest (ROI) selected for analysis was 5% of the femoral length from 0.1 mm below the growth plate to determine trabecular bone volume per tissue volume (Tb. BV/TV) and trabecular number (Tb. N). Tooth movement distance was measured between the two closest points from the sagittal view

with the smallest tooth distance. The length of the distal buccal root of the first molar was measured from the amelocemental junction to the root tip. Two trained researchers blinded to the group design independently measured tooth movement distance using ImageJ v.1.37 software (Wayne Rasband).

Tartrate-resistant acid phosphatase staining

The same sections used for histological study were deparaffinized and then used for TRAP staining. Cells were fixed in 4% paraformaldehyde and washed with PBS. The sections and cells were treated with TRAP with a leukocyte acid phosphatase kit (387A-1KT; Sigma, USA). According to the manufacturer's instructions, 0.5 mL Fast Garnet GBC base solution and 0.5 mL sodium nitrite solution were added to a tube, mixed by gentle inversion for 30 s, and allowed to stand for 2 min. The Diazotized Fast Garnet GBC solution was added in 45 mL of 37°C deionized water. The following solution was added to the deionized water: 0.5 mL Naphthol AS-Bl phosphate solution, 2.0 mL acetate solution, and 1.0 mL tartrate solution. Solutions were transferred from beakers to an appropriate Coplin jar. Solutions in jars were warmed to 37°C in a water bath. Slides were added to the Coplin jars and incubated for 1 h in a 37°C water bath protected from light. After 1 h, the slides were rinsed thoroughly in deionized water and then counterstained for 2 min in hematoxylin solution, Gill no. 3. Slides were rinsed for several minutes in alkaline tap water to reveal blue nuclei. The slides were air dried and evaluated microscopically. The TRAP-positive multinucleated (>3 nuclei) cells were counted in the PDL area adjacent to the alveolar bone, or the average number of TRAP-positive cells/mm^2 in each well of RAW264.7 macrophages was used.

Real-time PCR

Total RNA of the treated cells was extracted by TRIZOL reagent (Invitrogen, USA) and synthesis of cDNA was performed using the SuperScript RT-PCR system (Thermo Fisher Scientific, Rockford, IL, USA) with Platinum Taq High Fidelity (Invitrogen, USA). Quantitative real-time PCR was performed on a Real-Time PCR System (Applied Biosystems 7500, USA) using 2× SYBR Green (Invitrogen, USA). The primers used are listed in Table S2. The amplification specificity of the newly designed primers was confirmed by melting curve. Efficiency was confirmed by sequencing conventional PCR products.

Statistical analysis

Statistical analysis was performed by SPSS 22.0 software. Independent unpaired two-tailed Student's t tests were used to analyze the comparisons between two groups. In addition, one-way ANOVA with Tukey's tests was used to analyze the comparisons among more than two groups. A $p < 0.05$ was considered statistically significant.

Data availability

The datasets generated and analyzed during the current study are not publicly available due to the policy of the institution, but are available from the corresponding author on reasonable request.

SUPPLEMENTAL INFORMATION

Supplemental information can be found online at https://doi.org/10.1016/j.stemcr.2022.06.006.

AUTHOR CONTRIBUTIONS

The study was designed by Y.-H.Z., R.-L.Y., and H.-M.H.; H.-M.H. and C.-S.H. performed the experiments; S.-B.Z. helped with the mass data analysis; R.-L.Y. and H.-M.H. wrote the paper; S.-J.C., Y.-K.Z., T.-Y.X., and T.-Z. offered experimental advice; all authors analyzed data.

ACKNOWLEDGMENTS

This work was supported by the National Natural Science Foundation of China (81970940) (R.-L.Y.), Ten-thousand Talents Program (QNBJ-2020) (R.-L.Y.), and the National Science and Technology Major Project of the Ministry of Science and Technology of the People's Republic of China (2018ZX10302207). We thank the Facility for Protein Chemistry and Proteomics of Tsinghua University for the exosome proteomic profile analysis by LC-MS.

CONFLICT OF INTERESTS

The authors declare no competing interests.

Received: December 10, 2021
Revised: June 21, 2022
Accepted: June 22, 2022
Published: July 21, 2022

REFERENCES

Alexandre, C., and Vico, L. (2011). Pathophysiology of bone loss in disuse osteoporosis. Joint Bone Spine *78*, 572–576. https://doi.org/10.1016/j.jbspin.2011.04.007.

Balcerzak, M., Hamade, E., Zhang, L., Pikula, S., Azzar, G., Radisson, J., Bandorowicz-Pikula, J., and Buchet, R. (2003). The roles of annexins and alkaline phosphatase in mineralization process. Acta Biochim. Pol. *50*, 1019–1038. https://doi.org/10.18388/abp.2003_3629.

Bouter, A., Carmeille, R., Gounou, C., Bouvet, F., Degrelle, S.A., Evain-Brion, D., and Brisson, A.R. (2015). Review: annexin-A5 and cell membrane repair. Placenta *36*, S43–S49. https://doi.org/10.1016/j.placenta.2015.01.193.

Boyle, W.J., Simonet, W.S., and Lacey, D.L. (2003). Osteoclast differentiation and activation. Nature *423*, 337–342. https://doi.org/10.1038/nature01658.

Chinetti-Gbaguidi, G., Daoudi, M., Rosa, M., Vinod, M., Louvet, L., Copin, C., Fanchon, M., Vanhoutte, J., Derudas, B., Belloy, L., et al. (2017). Human alternative macrophages populate calcified areas of atherosclerotic lesions and display impaired RANKL-induced osteoclastic bone resorption activity. Circ. Res. *121*, 19–30. https://doi.org/10.1161/CIRCRESAHA.116.310262.

Colombo, M., Raposo, G., and Théry, C. (2014). Biogenesis, secretion, and intercellular interactions of exosomes and other extracellular vesicles. Annu. Rev. Cell Dev. Biol. *30*, 255–289. https://doi.org/10.1146/annurev-cellbio-101512-122326.

Diaz, M.F., Vaidya, A.B., Evans, S.M., Lee, H.J., Aertker, B.M., Alexander, A.J., Price, K.M., Ozuna, J.A., Liao, G.P., Aroom, K.R., et al. (2017). Biomechanical forces promote immune regulatory function of bone marrow mesenchymal stromal cells. Stem Cell. *35*, 1259–1272. https://doi.org/10.1002/stem.2587.

Ferguson, S.W., and Nguyen, J. (2016). Exosomes as therapeutics: the implications of molecular composition and exosomal heterogeneity. J. Control. Release *228*, 179–190. https://doi.org/10.1016/j.jconrel.2016.02.037.

Guo, C., Li, N., Dong, C., Wang, L., Li, Z., Liu, Q., Ma, Q., Greenaway, F.T., Tian, Y., Hao, L., et al. (2021). 33-kDa ANXA3 isoform contributes to hepatocarcinogenesis via modulating ERK, PI3K/Akt-HIF and intrinsic apoptosis pathways. J. Adv. Res. *30*, 85–102. https://doi.org/10.1016/j.jare.2020.11.003.

He, D., Kou, X., Yang, R., Liu, D., Wang, X., Luo, Q., Song, Y., Liu, F., Yan, Y., Gan, Y., and Zhou, Y. (2015). M1-like macrophage polarization promotes orthodontic tooth movement. J. Dent. Res. *94*, 1286–1294. https://doi.org/10.1177/0022034515589714.

Hessvik, N.P., and Llorente, A. (2018). Current knowledge on exosome biogenesis and release. Cell. Mol. Life Sci. *75*, 193–208. https://doi.org/10.1007/s00018-017-2595-9.

Hotokezaka, H., Sakai, E., Kanaoka, K., Saito, K., Matsuo, K.i., Kitaura, H., Yoshida, N., and Nakayama, K. (2002). U0126 and PD98059, specific inhibitors of MEK, accelerate differentiation of RAW264.7 cells into osteoclast-like cells. J. Biol. Chem. *277*, 47366–47372. https://doi.org/10.1074/jbc.M208284200.

Hsu, C., Morohashi, Y., Yoshimura, S.i., Manrique-Hoyos, N., Jung, S., Lauterbach, M.A., Bakhti, M., Grønborg, M., Möbius, W., Rhee, J., et al. (2010). Regulation of exosome secretion by Rab35 and its GTPase-activating proteins TBC1D10A-C. J. Cell Biol. *189*, 223–232. https://doi.org/10.1083/jcb.200911018.

Huang, H., Yang, R., and Zhou, Y.H. (2018). Mechanobiology of periodontal ligament stem cells in orthodontic tooth movement. Stem Cells Int. *2018*, 1–7. https://doi.org/10.1155/2018/6531216.

Jiang, N., Xiang, L., and He, L.; Yang, G., Zheng, J., Wang, C., Zhang, Y., Wang, S., Zhou, Y., Sheu, T.J., et al. (2017). Exosomes mediate epithelium–mesenchyme crosstalk in organ development. ACS Nano *11*, 7736–7746. https://doi.org/10.1021/acsnano.7b01087.

Johnstone, R.M. (1992). Maturation of reticulocytes: formation of exosomes as a mechanism for shedding membrane proteins. Biochem. Cell. Biol. *70*, 179–190. https://doi.org/10.1139/o92-028.

Karsdal, M.A., Bay-Jensen, A.C., Lories, R.J., Abramson, S., Spector, T., Pastoureau, P., Christiansen, C., Attur, M., Henriksen, K., Goldring, S.R., and Kraus, V. (2014). The coupling of bone and cartilage turnover in osteoarthritis: opportunities for bone antiresorptives and anabolics as potential treatments? Ann. Rheum. Dis. *73*, 336–348. https://doi.org/10.1136/annrheumdis-2013-204111.

Kowal, J., Tkach, M., and Théry, C. (2014). Biogenesis and secretion of exosomes. Curr. Opin. Cell Biol. *29*, 116–125. https://doi.org/10.1016/j.ceb.2014.05.004.

Kukita, T., Wada, N., Kukita, A., Kakimoto, T., Sandra, F., Toh, K., Nagata, K., Iijima, T., Horiuchi, M., Matsusaki, H., et al. (2004). RANKL-induced DC-STAMP is essential for osteoclastogenesis. J. Exp. Med. *200*, 941–946. https://doi.org/10.1084/jem.20040518.

Le, H.Q., Ghatak, S., Yeung, C.Y.C., Tellkamp, F., Günschmann, C., Dieterich, C., Yeroslaviz, A., Habermann, B., Pombo, A., Niessen, C.M., and Wickström, S.A. (2016). Mechanical regulation of transcription controls Polycomb-mediated gene silencing during lineage commitment. Nat. Cell Biol. *18*, 864–875. https://doi.org/10.1038/ncb3387.

LeBlanc, A.D., Spector, E.R., Evans, H.J., and Sibonga, J.D. (2007). Skeletal responses to space flight and the bed rest analog: a review. J. Musculoskelet. Neuronal Interact. *7*, 33–47.

Li, Y., Jacox, L.A., Little, S.H., and Ko, C.C. (2018a). Orthodontic tooth movement: the biology and clinical implications. Kaohsiung J. Med. Sci. *34*, 207–214. https://doi.org/10.1016/j.kjms.2018.01.007.

Li, Z., Fang, R., Fang, J., He, S., and Liu, T. (2018b). Functional implications of Rab27 GTPases in cancer. Cell Commun. Signal. *16*, 44. https://doi.org/10.1186/s12964-018-0255-9.

Liaw, N.Y., and Zimmermann, W.H. (2016). Mechanical stimulation in the engineering of heart muscle. Adv. Drug Deliv. Rev. *96*, 156–160. https://doi.org/10.1016/j.addr.2015.09.001.

Liu, F., Wen, F., He, D., Liu, D., Yang, R., Wang, X., Yan, Y., Liu, Y., Kou, X., and Zhou, Y. (2017). Force-induced H2S by PDLSCs modifies osteoclastic activity during tooth movement. J. Dent. Res. *96*, 694–702. https://doi.org/10.1177/0022034517690388.

Matsumoto, A., Takahashi, Y., Nishikawa, M., Sano, K., Morishita, M., Charoenviriyakul, C., Saji, H., and Takakura, Y. (2017). Role of phosphatidylserine-derived negative surface charges in the recognition and uptake of intravenously injected B16BL6-derived exosomes by macrophages. J. Pharm. Sci. *106*, 168–175. https://doi.org/10.1016/j.xphs.2016.07.022.

Menaa, C., Devlin, R.D., Reddy, S.V., Gazitt, Y., Choi, S.J., and Roodman, G.D. (1999). Annexin II increases osteoclast formation by stimulating the proliferation of osteoclast precursors in human marrow cultures. J. Clin. Invest. *103*, 1605–1613. https://doi.org/10.1172/JCI6374.

Mendt, M., Rezvani, K., and Shpall, E. (2019). Mesenchymal stem cell-derived exosomes for clinical use. Bone Marrow Transplant. *54*, 789–792. https://doi.org/10.1038/s41409-019-0616-z.

Moraes, C., Sun, Y., and Simmons, C.A. (2011). (Micro)managing the mechanical microenvironment. Integr. Biol. (Camb) *3*, 959. https://doi.org/10.1039/c1ib00056j.

Murphy, D.E., de Jong, O.G., Brouwer, M., Wood, M.J., Lavieu, G., Schiffelers, R.M., and Vader, P. (2019). Extracellular vesicle-based therapeutics: natural versus engineered targeting and trafficking. Exp. Mol. Med. *51*, 32. https://doi.org/10.1038/s12276-019-0223-5.

Ostrowski, M., Carmo, N.B., Krumeich, S., Fanget, I., Raposo, G., Savina, A., Moita, C.F., Schauer, K., Hume, A.N., Freitas, R.P., et al. (2010). Rab27a and Rab27b control different steps of the exosome secretion pathway. Nat. Cell Biol. *12*, 19–30. https://doi.org/10.1038/ncb2000.

Papachroni, K.K., Karatzas, D.N., Papavassiliou, K.A., Basdra, E.K., and Papavassiliou, A.G. (2009). Mechanotransduction in osteoblast regulation and bone disease. Trends Mol. Med. *15*, 208–216. https://doi.org/10.1016/j.molmed.2009.03.001.

Park, J.A., Sharif, A.S., Tschumperlin, D.J., Lau, L., Limbrey, R., Howarth, P., and Drazen, J.M. (2012). Tissue factor-bearing exosome

secretion from human mechanically stimulated bronchial epithelial cells in vitro and in vivo. J. Allergy Clin. Immunol. *130*, 1375–1383. https://doi.org/10.1016/j.jaci.2012.05.031.

Pironti, G., Strachan, R.T., Abraham, D., Mon-Wei Yu, S., Chen, M., Chen, W., Hanada, K., Mao, L., Watson, L.J., and Rockman, H.A. (2015). Circulating exosomes induced by cardiac pressure overload contain functional angiotensin II type 1 receptors. Circulation *131*, 2120–2130. https://doi.org/10.1161/CIRCULATIONAHA.115.015687.

Rana, S., Yue, S., Stadel, D., and Zöller, M. (2012). Toward tailored exosomes: the exosomal tetraspanin web contributes to target cell selection. Int. J. Biochem. Cell Biol. *44*, 1574–1584. https://doi.org/10.1016/j.biocel.2012.06.018.

Sadvakassova, G., Tiedemann, K., Steer, K.J.D., Mikolajewicz, N., Stavnichuk, M., In-Kyung Lee, I., Sabirova, Z., Schranzhofer, M., and Komarova, S.V. (2021). Active hematopoiesis triggers exosomal release of PRDX2 that promotes osteoclast formation. Physiol. Rep. *9*, e14745. https://doi.org/10.14814/phy2.14745.

Seo, B.M., Miura, M., Gronthos, S., Mark Bartold, P., Batouli, S., Brahim, J., Young, M., Gehron Robey, P., Wang, C.Y., and Shi, S. (2004). Investigation of multipotent postnatal stem cells from human periodontal ligament. Lancet *364*, 149–155. https://doi.org/10.1016/S0140-6736(04)16627-0.

Sun, X., Shu, Y., Xu, M., Jiang, J., Wang, L., Wang, J., Huang, D., and Zhang, J. (2020). ANXA6 suppresses the tumorigenesis of cervical cancer through autophagy induction. Clin. Transl. Med. *10*, e208. https://doi.org/10.1002/ctm2.208.

Tamma, R., Colaianni, G., Camerino, C., Di Benedetto, A., Greco, G., Strippoli, M., Vergari, R., Grano, A., Mancini, L., Mori, G., et al. (2009). Microgravity during spaceflight directly affects in vitro osteoclastogenesis and bone resorption. FASEB J. *23*, 2549–2554. https://doi.org/10.1096/fj.08-127951.

Teichtahl, A.J., Wluka, A.E., Wijethilake, P., Wang, Y., Ghasem-Zadeh, A., and Cicuttini, F.M. (2015). Wolff's law in action: a mechanism for early knee osteoarthritis. Arthritis Res. Ther. *17*, 207. https://doi.org/10.1186/s13075-015-0738-7.

Tiedemann, K., Sadvakassova, G., Mikolajewicz, N., Juhas, M., Sabirova, Z., Tabariès, S., Gettemans, J., Siegel, P.M., and Komarova, S.V. (2019). Exosomal release of L-plastin by breast cancer cells facilitates metastatic bone osteolysis. Transl. Oncol. *12*, 462–474. https://doi.org/10.1016/j.tranon.2018.11.014.

Tkach, M., and Théry, C. (2016). Communication by extracellular vesicles: where we are and where we need to go. Cell *164*, 1226–1232. https://doi.org/10.1016/j.cell.2016.01.043.

Tschumperlin, D.J., Dai, G., Maly, I.V., Kikuchi, T., Laiho, L.H., McVittie, A.K., Haley, K.J., Lilly, C.M., So, P.T.C., Lauffenburger, D.A., et al. (2004). Mechanotransduction through growth-factor shedding into the extracellular space. Nature *429*, 83–86. https://doi.org/10.1038/nature02543.

Wada, N., Menicanin, D., Shi, S., Bartold, P.M., and Gronthos, S. (2009). Immunomodulatory properties of human periodontal ligament stem cells. J. Cell. Physiol. *219*, 667–676. https://doi.org/10.1002/jcp.21710.

Wang, Z., Maruyama, K., Sakisaka, Y., Suzuki, S., Tada, H., Suto, M., Saito, M., Yamada, S., and Nemoto, E. (2019). Cyclic stretch force induces periodontal ligament cells to secrete exosomes that suppress IL-1β production through the inhibition of the NF-κB signaling pathway in macrophages. Front. Immunol. *10*, 1310. https://doi.org/10.3389/fimmu.2019.01310.

Wang, L., You, X., Zhang, L., Zhang, C., and Zou, W. (2022). Mechanical regulation of bone remodeling. Bone Res. *10*, 16. https://doi.org/10.1038/s41413-022-00190-4.

Wei, Y., Wang, D., Jin, F., Bian, Z., Li, L., Liang, H., Li, M., Shi, L., Pan, C., Zhu, D., et al. (2017). Pyruvate kinase type M2 promotes tumour cell exosome release via phosphorylating synaptosome-associated protein 23. Nat. Commun. *8*, 14041. https://doi.org/10.1038/ncomms14041.

Yi, Y.W., Lee, J.H., Kim, S.Y., Pack, C.G., Ha, D.H., Park, S.R., Youn, J., and Cho, B.S. (2020). Advances in analysis of biodistribution of exosomes by molecular imaging. Int. J. Mol. Sci. *21*, 665. https://doi.org/10.3390/ijms21020665.

Yuan, J., Liu, H., Gao, W., Zhang, L., Ye, Y., Yuan, L., Ding, Z., Wu, J., Kang, L., Zhang, X., et al. (2018). MicroRNA-378 suppresses myocardial fibrosis through a paracrine mechanism at the early stage of cardiac hypertrophy following mechanical stress. Theranostics *8*, 2565–2582. https://doi.org/10.7150/thno.22878.

Zhang, X., Yuan, X., Shi, H., Wu, L., Qian, H., and Xu, W. (2015). Exosomes in cancer: small particle, big player. J. Hematol. Oncol. *8*, 83. https://doi.org/10.1186/s13045-015-0181-x.

Zhang, L., Liu, W., Zhao, J., Ma, X., Shen, L., Zhang, Y., Jin, F., and Jin, Y. (2016). Mechanical stress regulates osteogenic differentiation and RANKL/OPG ratio in periodontal ligament stem cells by the Wnt/β-catenin pathway. Biochim. Biophys. Acta *1860*, 2211–2219. https://doi.org/10.1016/j.bbagen.2016.05.003.